Quadrupole transitions in the bound rotational-vibrational spectrum of the hydrogen molecular ion

Horacio Olivares Pilón and Daniel Baye

Physique Quantique C.P. 165/82, and Physique Nucléaire Théorique et Physique Mathématique, C.P. 229, Université Libre de Bruxelles (ULB), B 1050 Brussels, Belgium

E-mail: dbaye@ulb.ac.be

Abstract. The three-body Schrödinger equation of the H_2^+ hydrogen molecular ion with Coulomb potentials is solved in perimetric coordinates using the Lagrange-mesh method. The Lagrange-mesh method is an approximate variational calculation with variational accuracy and the simplicity of a calculation on a mesh. Energies and wave functions of up to four of the lowest vibrational bound or quasibound states for total orbital momenta from 0 to 40 are calculated. The obtained energies have an accuracy varying from about 13 digits for the lowest vibrational state to at least 9 digits for the third vibrational excited state. With the corresponding wave functions, a simple calculation using the associated Gauss quadrature provides accurate quadrupole transition probabilities per time unit between those states over the whole rotational bands. Extensive results are presented with six significant figures.

PACS numbers: 31.15.Ag, 31.15.Ac, 02.70.Hm, 02.70.Jn

Submitted to: *J. Phys. B: At. Mol. Opt. Phys.*

2 February 2012

1. Introduction

The H_2^+ bound rotational-vibrational spectrum possesses about 420 bound states corresponding to the Σ_g electronic configuration as well as about 60 narrow quasibound levels. For this simple three-body system, the Schrödinger equation involving Coulomb potentials can not be solved exactly but it is possible to reach a high accuracy for both energies and wave functions. A calculation of the energies of most rotational-vibrational bound states and some quasi-bound levels has been performed in 1993 with 11-digit accuracy by Moss [1]. He also calculated energies for the few extended bound Σ_u states. Since then, several calculations have reached a higher accuracy, but always for a limited number of bound states. The energy of the ground state, with total orbital momentum $L = 0$ and positive parity, has been improved in a number of papers [2, 3, 4, 5, 6, 7, 8] to reach an accuracy around or beyond 30 digits [7, 8]. The energy of the first $L = 0$ excited state has also been improved [6, 8]. The lowest $L = 1$ vibrational state has been considered by several authors [5, 6, 7, 8]. The $L = 0$ and 1 excited vibrational states have been studied by Hilico *et al* [3] (see also [9]). Energies of the full ground-state rotational band were determined with 12-digit accuracy by Hesse and Baye [10] and energies up to $L = 12$ with higher accuracy were obtained by Yan and Zhang [11]. Some of the quoted works also provide accurate information on mean radii [10, 8] or quadrupole moments [10].

In opposition to this large number of accurate studies, very few studies concern the transition probabilities between the rotational-vibrational bound states of H_2^+. There are several reasons for this. As the electric dipole transitions are forbidden by the symmetry the two protons, the more complicated electric quadrupole transitions are the dominant mode of decay. Moreover, few existing studies provide the necessary wave functions. Since the pioneering work of Bates and Poots [12], a systematic study of all transitions for states up to $L = 20$ within the Born-Oppenheimer approximation has been published with two significant figures [13]. Here we present accurate E2 transition probabilities without Born-Oppenheimer approximation. They are obtained from three-body wave functions calculated with the Lagrange-mesh method in perimetric coordinates [14, 15, 10], with which the calculation is particularly simple and very precise.

The Lagrange-mesh method is an approximate variational calculation using a basis of Lagrange functions and the associated Gauss quadrature. It has the high accuracy of a variational approximation and the simplicity of a calculation on a mesh. Lagrange functions are N orthonormal infinitely differentiable functions that vanish at all points of this mesh, except one. Used as a variational basis in a quantum-mechanical calculation, the Lagrange functions lead to a simple approximation when matrix elements are calculated with the associated Gauss quadrature. The variational equations take the form of mesh equations with a diagonal representation of the potential only depending on values of this potential at the mesh points [16, 17]. The most striking property of the Lagrange-mesh method is that, in spite of its simplicity, the obtained energies and

wave functions can be as accurate with the Gauss quadrature approximation as in the original variational method with an exact calculation of the matrix elements [18, 17]. The accuracy of the lowest energies exceeds by far the accuracy of the Gauss quadrature for the individual matrix elements. The Lagrange-mesh method allows very accurate calculations not only in simple quantum-mechanical problems but also in various more complicated applications in atomic [19, 20, 21], molecular [14, 15, 10, 22, 23] and nuclear [24, 25, 26] physics.

In the H_2^+ case, the Lagrange-mesh method is applied in perimetric coordinates, i.e. three angles describing the orientation of the plane containing the particles and three linear combinations of the distances between them [27]. The dependence on the three Euler angles is treated analytically [15, 10]. The three perimetric coordinates vary from zero to infinity and can easily be discretized on a three-dimensional Lagrange-Laguerre mesh [14]. An additional advantage is that the resulting matrix is rather sparse. The Lagrange-mesh method also provides analytical approximations for the wave functions that lead to very simple expressions for a number of matrix elements when used with the corresponding Gauss-Laguerre quadrature.

In section 2, the basic expressions for the transition probabilities are recalled. The E1 and E2 operators are expressed in perimetric coordinates. Some definitions about Lagrange functions lead to Lagrange-mesh expressions for the transition matrix elements. In section 3, energies are given for the lowest four vibrational states over the full rotational bands and E2 transition probabilities are tabulated. Concluding remarks are presented in section 4.

2. Lagrange-mesh calculation of transition probabilities

2.1. Oscillator strength and transition probability per time unit

The dimensionless oscillator strength for an electric transition of multipolarity λ between an initial state i and a final state f is defined as [28, 29]

$$f_{i\to f}^{(\lambda)} = \frac{m_e c}{\hbar} \frac{(2\lambda+1)(\lambda+1)}{[(2\lambda+1)!!]^2 \lambda} k^{2\lambda-1} \frac{S_{if}^{(\lambda)}}{2J_i+1} \tag{1}$$

where m_e is the electron mass,

$$k = \frac{|E_f - E_i|}{\hbar c} \tag{2}$$

is the photon wavenumber and

$$S_{if}^{(\lambda)} = S_{fi}^{(\lambda)} = \sum_{M_i M_f \mu} |\langle \gamma_i J_i M_i | O_\mu^{(\lambda)} | \gamma_f J_f M_f \rangle|^2 = |\langle \gamma_i J_i || O^{(\lambda)} || \gamma_f J_f \rangle|^2, \tag{3}$$

where $J_{i,f}$ is a total angular momentum, $M_{i,f}$ is its projection, $\gamma_{i,f}$ represents the other quantum numbers and the reduced matrix element is defined according to [30]. The transition irreducible tensor operator is given in units of e by

$$O_\mu^{(\lambda)} = \sum_i Z_i r_i'^\lambda C_\mu^{(\lambda)}(\Omega_i') \tag{4}$$

where $\boldsymbol{r}'_i = \boldsymbol{r} - \boldsymbol{R}_{\rm c.m.}$ is the relative coordinate of particle i with respect to the center of mass, Z_i is its charge in units of e and $C^{(\lambda)}_\mu(\Omega) = \sqrt{4\pi/(2\lambda+1)}Y^{(\lambda)}_\mu(\Omega)$. Notice that the charge unit e is included in the coefficient in $f^{(\lambda)}_{i\to f}$. One has

$$f^{(\lambda)}_{f\to i} = \frac{2J_i+1}{2J_f+1} f^{(\lambda)}_{i\to f}. \tag{5}$$

If atomic units are used, the oscillator strength reads

$$f^{(\lambda)}_{i\to f} = \frac{(2\lambda+1)(\lambda+1)}{[(2\lambda+1)!!]^2\lambda}\alpha^{2\lambda-2}\left(E_f - E_i\right)^{2\lambda-1}\frac{S^{(\lambda)}_{if}}{2J_i+1} \tag{6}$$

where α is the fine-structure constant.

The transition probability per time unit for $E_f < E_i$ is given in atomic units (the atomic unit of time is $a_0/\alpha c \approx 2.4188843 \times 10^{-17}$ s) by

$$W^{(\lambda)}_{i\to f} = \frac{2(\lambda+1)(2\lambda+1)}{\lambda[(2\lambda+1)!!]^2}\alpha^{2\lambda+1}(E_i - E_f)^{2\lambda+1}\frac{S^{(\lambda)}_{if}}{2J_i+1} \tag{7}$$

where all quantities are in a.u. For any multipolarity λ, the transition probability is related to the oscillator strength by

$$W^{(\lambda)}_{i\to f} = 2\alpha^3(E_i - E_f)^2 f^{(\lambda)}_{i\to f}. \tag{8}$$

2.2. Dipole and quadrupole operators in perimetric coordinates

After elimination of the centre-of-mass motion, the Hamiltonian depends on the two Jacobi coordinates $\boldsymbol{R}$ of proton 2 with respect to proton 1 and $\boldsymbol{r}$ of the electron with respect to the centre of mass of both protons. These coordinates can be expressed as three Euler angles (ψ, θ, ϕ) defining the orientation of the triangle formed by the three particles, and three internal coordinates describing the shape of this triangle. The θ and ψ angles correspond to the angular spherical coordinates of vector $\boldsymbol{R} = (R, \theta, \psi)$ and the ϕ angle is the angular cylindrical coordinate of vector $\boldsymbol{r} = (\rho, \zeta, \phi)$ in the relative frame where the z-axis is moved along $\boldsymbol{R}$ by ψ and θ rotations [31]. For the internal degrees of freedom we use the perimetric coordinates (x, y, z) defined as linear combinations of interparticle distances [27],

$$\begin{aligned} x &= R - r_{e2} + r_{e1}, \\ y &= R + r_{e2} - r_{e1}, \\ z &= -R + r_{e2} + r_{e1}, \end{aligned} \tag{9}$$

where r_{e1} and r_{e2} are the distances between the electron and protons 1 and 2, respectively. The domains of variation of these six variables are $[0, 2\pi]$ for ψ and ϕ, $[0, \pi]$ for θ and $[0, \infty[$ for x, y and z.

In the body-fixed frame, the radial component of $\boldsymbol{R}$ and the polar and axial components of $\boldsymbol{r}$ are expressed in perimetric coordinates (9) as [15, 10]

$$R = \frac{x+y}{2}, \tag{10}$$

$$\rho = \sqrt{\frac{xyz(x+y+z)}{(x+y)^2}}, \tag{11}$$

$$\zeta = \frac{(x-y)(2z+x+y)}{4(x+y)}. \tag{12}$$

For H_2^+, the dipole tensor operator reads in Jacobi coordinates,

$$d_\mu^{(1)} = -\left(1+\frac{m_e}{M}\right) r_\mu^{(1)} \tag{13}$$

where $M = 2m_p + m_e$ is the total mass of the molecular ion. This operator changes sign under space reflection (odd operator). It is invariant under the permutation of the protons. The tensor components of $\boldsymbol{r}$ can be written as a function of the Euler angles (ψ, θ, ϕ) as

$$r_\mu^{(1)} = \zeta D_{\mu 0}^1(\psi,\theta,\phi) + \frac{\rho}{\sqrt{2}}[D_{\mu 1}^1(\psi,\theta,\phi) - D_{\mu -1}^1(\psi,\theta,\phi)]. \tag{14}$$

In both terms, the Wigner matrices change sign under space reflection [15] while ζ and ρ remain unchanged. With respect to proton exchange [15], ζ and $D_{\mu 0}^1$ are both odd while ρ and $D_{\mu 1}^1 - D_{\mu -1}^1$ are both even.

In the Jacobi coordinate system, the E2 tensor operator reads

$$Q_\mu^{(2)} = \sqrt{\frac{3}{2}}\left\{\frac{1}{2}[R^{(1)} \otimes R^{(1)}]_\mu^{(2)} - \gamma[r^{(1)} \otimes r^{(1)}]_\mu^{(2)}\right\} \tag{15}$$

where

$$\gamma = 1 - \frac{2m_e}{M} - \frac{m_e^2}{M^2}. \tag{16}$$

In perimetric coordinates, it becomes

$$Q_\mu^{(2)} = \frac{1}{2}[R^2 - \gamma(2\zeta^2 - \rho^2)]D_{\mu 0}^2(\psi,\theta,\phi) - \sqrt{\frac{3}{2}}\gamma\zeta\rho[D_{\mu 1}^2(\psi,\theta,\phi) - D_{\mu -1}^2(\psi,\theta,\phi)]$$
$$-\sqrt{\frac{3}{8}}\gamma\rho^2[D_{\mu 2}^2(\psi,\theta,\phi) + D_{\mu -2}^2(\psi,\theta,\phi)]. \tag{17}$$

Operator $Q_\mu^{(2)}$ is even with respect to parity and to permutation.

2.3. Transition matrix elements

The three-body Hamiltonian that we consider involves Coulomb forces between the particles but no spin-dependent forces. Hence the total orbital momentum L and parity π are good quantum numbers corresponding to constants of motion. The wave functions with orbital momentum L and parity π are expanded as [10]

$$\Psi_M^{(L^\pi)\sigma} = \sum_{K=0}^{L} \mathcal{D}_{MK}^{L\pi}(\psi,\theta,\phi)\Phi_K^{(L^\pi)\sigma}(x,y,z). \tag{18}$$

In practice, the sum can be truncated at some value $K_{\max}$. The normalized angular functions $\mathcal{D}_{MK}^{L\pi}(\psi,\theta,\phi)$ are defined for $K \geq 0$ by

$$\mathcal{D}_{MK}^{L\pi}(\psi,\theta,\phi) = \frac{\sqrt{2L+1}}{4\pi}\left(1+\delta_{K0}\right)^{-1/2}\left[D_{MK}^L(\psi,\theta,\phi)\right.$$
$$\left.+\pi(-1)^{L+K}D_{M\,-K}^L(\psi,\theta,\phi)\right] \tag{19}$$

where $D^L_{MK}(\psi,\theta,\phi)$ represents a Wigner matrix element. They have parity π and change as $\pi(-1)^K$ under permutation of the protons. Hence $\Phi_K^{(L^\pi)\sigma}$ is symmetric for $(-1)^K=\sigma\pi$ and antisymmetric for $(-1)^K=-\sigma\pi$, when x and y are exchanged. Most bound states belong to the Σ_g band where $K=0$ dominates and σ is equal to π.

Since the symmetry of the proton spin part is $(-1)^{S+1}$ where S is the total spin of the protons, physical states (i.e. states antisymmetric with respect to the exchange of the protons) have $\sigma=(-1)^S$. In the Σ_g rovibrational band, states have natural parity, $\pi=\sigma=(-1)^L$. Even-L states have positive parity and $\sigma=+1$. The protons are thus in a singlet state and the total intrinsic spin of the molecule is 1/2. Odd-L states have negative parity and $\sigma=-1$. The protons are in a triplet state and the total intrinsic spin of the molecule is 1/2 or 3/2. E1 transitions are forbidden because of different proton symmetries when $\Delta L=1$. However, they are possible from the three weakly bound states of the Σ_u band where $\pi=\sigma=(-1)^{L+1}$. E2 transitions are possible within the Σ_g rovibrational band for $\Delta L=0,\pm2$. Such states have the same parity and symmetry.

Using the property

$$\langle D^{L'}_{M'K'}|D^\lambda_{\mu\kappa}|D^L_{MK}\rangle=\frac{8\pi^2}{2L'+1}(L\lambda M\mu|L'M')(L\lambda K\kappa|L'K'),\tag{20}$$

one can write for $\kappa\geq0$,

$$\begin{aligned}F^{LL';\lambda}_{KK';\kappa}&=\langle\mathcal{D}^{L'\pi'}_{M'K'}|D^\lambda_{\mu\kappa}+(-1)^\kappa D^\lambda_{\mu-\kappa}|\mathcal{D}^{L\pi}_{MK}\rangle\\&=\frac{(2L+1)^{1/2}}{[(2L'+1)(1+\delta_{K'0})(1+\delta_{K0})]^{1/2}}(L\lambda M\mu|L'M')\\&\times\{(L\lambda K\kappa|L'K')+(-1)^\kappa(L\lambda K\,-\kappa|L'K')\\&+\pi'(-1)^{L'+K'}[(L\lambda K\kappa|L'\,-K')+(-1)^\kappa(L\lambda K\,-\kappa|L'\,-K')]\}.\end{aligned}\tag{21}$$

The reduced matrix elements of the operators $Q^{(2)}_\mu$ between initial and final states $\Psi^{i(L_i^{\pi_i})\sigma_i}_{M_i}$ and $\Psi^{f(L_f^{\pi_f})\sigma_f}_{M_f}$ can be written as

$$\langle\Psi^{f(L_f^{\pi_f})\sigma_f}||Q^{(2)}||\Psi^{i(L_i^{\pi_i})\sigma_i}\rangle=\sum_{K_iK_f}\sum_{\kappa=0}^{2}(1+\delta_{\kappa0})^{-1}F^{L_iL_f;2}_{K_iK_f;\kappa}A^{L_iL_f}_{K_iK_f;\kappa}\tag{22}$$

where the perimetric matrix elements

$$A^{L_iL_f}_{K_iK_f;\kappa}=\langle\Phi^{f(L_f^{\pi_f})\sigma_f}_{K_f}|\mathcal{A}_\kappa|\Phi^{i(L_i^{\pi_i})\sigma_i}_{K_i}\rangle\tag{23}$$

are calculated by integration over the perimetric coordinates with the volume element $(x+y)(y+z)(z+x)dxdydz$ and, from (17),

$$\mathcal{A}_0=\frac{1}{2}[R^2-\gamma(2\zeta^2-\rho^2)],\quad\mathcal{A}_1=-\sqrt{\frac{3}{2}}\gamma\zeta\rho,\quad\mathcal{A}_2=-\sqrt{\frac{3}{8}}\gamma\rho^2,\tag{24}$$

with R, ρ and ζ replaced by their expressions (10)-(12). With (3) and (22), the oscillator strength is given explicitly for transitions between natural-parity states $\pi_{i,f}=(-1)^{L_{i,f}}$ by

$$S^{(2)}_{if}=(2L_i+1)\Big|\sum_{K_iK_f}\Big\{C^{L_i2L_f}_{K_i0K_f}A^{L_iL_f}_{K_iK_f;0}$$

$$+\left[C^{L_i 2L_f}_{K_i 1 K_f}(1+\delta_{K_i 0})^{1/2} - C^{L_i 2L_f}_{K_i-1 K_f}(1+\delta_{K_f 0})^{1/2}\right] A^{L_i L_f}_{K_i K_f;1}$$
$$+\left[C^{L_i 2L_f}_{K_i 2 K_f}(1+\delta_{K_i 0})^{1/2} + C^{L_i 2L_f}_{K_i-2 K_f}(1+\delta_{K_f 0})^{1/2} - C^{L_i 2L_f}_{2-1 1}\delta_{K_i 1}\delta_{K_f 1}\right] A^{L_i L_f}_{K_i K_f;2}\Big\}\Big|^2 \quad (25)$$

where the Clebsch-Gordan coefficients are written as $C^{L_i\lambda L_f}_{K_i\mu K_f} = (L_i\lambda K_i\mu|L_f K_f)$ and the sums over K_i and K_f are truncated at $K_{\max}$ in practice. The remaining calculation of the matrix elements $A^{L_i L_f}_{K_i K_f;\kappa}$ is particularly simple within the Lagrange-mesh method as shown in the next subsection.

2.4. Lagrange-mesh method

The three-dimensional Lagrange functions $F^K_{ijk}(x,y,z)$ are infinitely differentiable functions defined by

$$F^K_{ijk}(x,y,z) = \mathcal{N}^{-1/2}_{Kijk}\mathcal{R}_K(x,y,z) f_i^{N_x}(x/h_x) f_j^{N_y}(y/h_y) f_k^{N_z}(z/h_z). \quad (26)$$

The one-dimensional Lagrange-Laguerre functions f_i^N are given by

$$f_i^N(u) = (-1)^i u_i^{1/2}\frac{L_N(u)}{u-u_i}e^{-u/2} \quad (27)$$

where $L_N(u)$ is the Laguerre polynomial of degree N and u_i is one of its zeros, i.e. $L_N(u_i) = 0$. They vanish at all u_j with $j \neq i$. Basis (26) is exactly equivalent to the set of functions $\mathcal{R}_K(x,y,z)L_{n_x}(x/h_x)L_{n_y}(y/h_y)L_{n_z}(z/h_z)\exp[-(x/2h_x)-(y/2h_y)-(z/2h_z)]$ with $n_{x,y,z} = 0$ to $N_{x,y,z} - 1$. The mesh points $(h_x u_p, h_y v_q, h_z w_r)$ correspond to the zeros u_p, v_q, w_r of Laguerre polynomials of respective degrees N_x, N_y, N_z. Three scale parameters h_x, h_y, h_z are introduced in (26) in order to fit the different meshes to the size of the actual physical problem. The function $\mathcal{R}_K(x,y,z)$ is a regularization factor introduced because of the presence of singularities in the Hamiltonian operator when L differs from zero [15, 10]. It is equal to 1 when $K = 0$ and to $\sqrt{xyz(x+y+z)}$ otherwise. The normalization factor $\mathcal{N}_{Kijk}$ is defined as

$$\mathcal{N}_{Kijk} = h_x h_y h_z (h_x u_i + h_y v_j)(h_x u_i + h_z w_k)(h_y v_j + h_z w_k)\mathcal{R}^2_{Kijk} \quad (28)$$

where $\mathcal{R}_{Kijk} = \mathcal{R}_K(h_x u_i, h_y v_j, h_z w_k)$.

The functions $F^K_{ijk}(x,y,z)$ satisfy the Lagrange property with respect to the three-dimensional mesh $(h_x u_p, h_y v_q, h_z w_r)$, i.e. they vanish at all mesh points but one,

$$F^K_{ijk}(h_x u_p, h_y v_q, h_z w_r) = (\mathcal{N}_{Kijk}\mathcal{R}^{-2}_{Kijk}\lambda_i^{N_x}\lambda_j^{N_y}\lambda_k^{N_z})^{-1/2}\delta_{ip}\delta_{jq}\delta_{kr}. \quad (29)$$

The coefficients $\lambda_i^{N_x}$, $\lambda_j^{N_y}$, $\lambda_k^{N_z}$ are the Christoffel numbers which appear as weights in the Gauss-Laguerre quadrature approximation

$$\int_0^\infty\int_0^\infty\int_0^\infty G(u,v,w)dudvdw \approx \sum_{i=1}^{N_x}\sum_{j=1}^{N_y}\sum_{k=1}^{N_z}\lambda_i^{N_x}\lambda_j^{N_y}\lambda_k^{N_z}G(u_i,v_j,w_k). \quad (30)$$

At the Gauss approximation scaled with h_x, h_y, h_z, the three-dimensional Lagrange functions (26) are orthonormal with respect to the perimetric volume element because of the Lagrange property (29).

The $\Phi_K^{(L^\pi)\sigma}(x,y,z)$ functions of equation (18) are expanded in the Lagrange basis as

$$\Phi_K^{(L^\pi)\sigma}(x,y,z) = \sum_{i=1}^{N}\sum_{j=1}^{i-\delta_K}\sum_{k=1}^{N_z} C_{Kijk}^{(L^\pi)\sigma}\,[2(1+\delta_{ij})]^{-1/2} \times \left[F_{ijk}^K(x,y,z) + \sigma\pi(-1)^K F_{jik}^K(x,y,z)\right] \tag{31}$$

where we use the same number N of mesh points and the same scale factor h for the two perimetric coordinates x and y in order to take advantage of the Lagrange conditions (29) when the two coordinates are exchanged. Because of the symmetrization the sum over j is limited by the value $i-\delta_K$, where δ_K is equal to 0 when $(-1)^K = \sigma\pi$ and to 1 when $(-1)^K = -\sigma\pi$.

The three-body Hamiltonian in perimetric coordinates for each good quantum number L and its discretization on a Lagrange mesh are given in [15]. The singularities of the three Coulomb terms are automatically regularized in the matrix elements by the volume element so that the Lagrange-mesh method is not affected by those singularities. The potential matrix is diagonal and its elements are the values of the potential at the mesh points. The calculation would be as easy with other form factors for the potentials. The resulting matrix is rather sparse. The remaining problem is to calculate the lowest eigenvalues and the corresponding eigenvectors of a large sparse matrix.

For given L^π, the eigenvalues in increasing order are labeled by a quantum number $v \geq 0$ related to the vibrational excitation in the Born-Oppenheimer picture. The corresponding eigenvectors provide the coefficients appearing in expansion (31).

Let us consider initial and final components (31) with respective coefficients $C_{K_iijk}^{i(L_i^{\pi_i})\sigma_i}$ and $C_{K_fijk}^{f(L_f^{\pi_f})\sigma_f}$. Because of the Lagrange property (29), the matrix elements (23) are simply obtained with the Gauss quadrature (30) as

$$A_{K_iK_f;\kappa}^{L_iL_f} \approx \sum_{i=1}^{N}\sum_{j=1}^{i-\delta_K}\sum_{k=1}^{N_z} C_{K_iijk}^{i(L_i^{\pi_i})\sigma_i} C_{K_fijk}^{f(L_f^{\pi_f})\sigma_f} \mathcal{A}_\kappa(hu_i, hv_j, h_z w_k) \tag{32}$$

where $\delta_K = \max(\delta_{K_i}, \delta_{K_f})$.

3. Energies and E2 transition probabilities

3.1. H_2^+ bound and quasibound energies

The energies of the $v = 0$ lowest vibrational bound states for $L = 0$ to 35 have been calculated with the present method in [10]. Here we extend those calculations to quasibound states up to $L = 40$ and to the first three excited vibrational states. The main reason making this extension possible is a better technique for searching the eigenvalues of a large sparse matrix [32] and faster personal computers.

Since the main aim is to calculate transition matrix elements involving two different wave functions, it is convenient to use a single three-dimensional mesh for all states. An excellent accuracy is obtained when the parameters of the calculation are chosen as

$N = N_x = N_y = 40$, $N_z = 20$ and $h = h_x = h_y = 0.14$, $h_z = 0.4$. For a given K value, the total number of basis states is then 16400 or 15600 depending on the parity of K. The size of the matrix is larger by about a factor $(K_{\max} + 1)$ when K is limited by $K \leq K_{\max} \leq L$. For $K > 2$, like in [10], calculations are performed with $K_{\max} = 2$. They correspond to a size of 48400. In order to make comparisons with more accurate literature results, we use for the proton mass the benchmark value $m_p = 1836.152701$ a.u. The dissociation threshold E_d is then at $-0.499\,727\,839\,716$ a.u. or Hartrees. The obtained energies are presented as the first line for each L value in Table 1. The accuracy is estimated from the stability of the digits with respect to calculations with $N \pm 2$ mesh points. The error is expected to be at most of a few units on the last displayed digit. Literature results sometimes truncated at the 15th digit are displayed in each second line. Except in the low-L or low v regions where other references are mentioned, the literature results are the 11-digit energies obtained by Moss [1].

Table 1: Energies of the four lowest vibrational bound or quasibound states in the Σ_g rotational band of the H_2^+ molecular ion. Quasibound states are separated from bound states by a horizontal bar. For each L value, the Lagrange-mesh results obtained with $N_x = N_y = 40$, $N_z = 20$ and $h_x = h_y = 0.14$, $h_z = 0.4$ are presented in the first line. The second line displays the results of Moss [1] except when other references are indicated (^{a}: [8], ^{b}: [7], ^{c}: [3], ^{d}: [11]). For $L = 0$, Lagrange-mesh results obtained with $N = 55$, $N_z = 25$ are given in the third line. The proton mass is taken as $m_p = 1836.152701 m_e$.

L	$v = 0$	$v = 1$	$v = 2$	$v = 3$
0	-0.597 139 063 123 3	-0.587 155 679 207	-0.577 751 904 49	-0.568 908 497 8
	-0.597 139 063 123 405^{a,b}	-0.587 155 679 212 747^b	-0.577 751 904 595 47^c	-0.568 908 498 966 77^c
	-0.597 139 063 123 41	-0.587 155 679 212 76	-0.577 751 904 595 47	-0.568 908 498 966 75
1	-0.596 873 738 832 6	-0.586 904 321 034	-0.577 514 034 14	-0.568 683 707 4
	-0.596 873 738 832 765^{a,b}	-0.586 904 321 04^c	-0.577 514 034 24^c	-0.568 683 708 50^c
2	-0.596 345 205 545 3	-0.586 403 631 650	-0.577 040 237 25	-0.568 235 992 1
	-0.596 345 205 545 46^d	-0.586 403 631 64	-0.577 040 237 32	-0.568 235 993 18
3	-0.595 557 639 048 1	-0.585 657 612 010	-0.576 334 350 31	-0.567 569 033 9
	-0.595 557 639 048 23^d	-0.585 657 612 02	-0.576 334 350 40	-0.567 569 035 05
4	-0.594 517 169 322 3	-0.584 672 134 376	-0.575 402 003 40	-0.566 688 235 7
	-0.594 517 169 322 41^d	-0.584 672 134 39	-0.575 402 003 51	-0.566 688 236 89
5	-0.593 231 728 998 2	-0.583 454 796 107	-0.574 250 479 24	-0.565 600 585 3
	-0.593 231 728 998 34^d	-0.583 454 796 10	-0.574 250 479 35	-0.565 600 586 54
6	-0.591 710 865 102 0	-0.582 014 738 323	-0.572 888 538 69	-0.564 314 488 1

Continued on Next Page...

Table 1 – Continuation

L	$v=0$	$v=1$	$v=2$	$v=3$
	-0.591 710 865 102 11^d	-0.582 014 738 32	-0.572 888 538 80	-0.564 314 489 33
7	-0.589 965 524 077 8	-0.580 362 439 246	-0.571 326 222 24	-0.562 839 576 1
	-0.589 965 524 077 97^d	-0.580 362 439 24	-0.571 326 222 33	-0.562 839 577 36
8	-0.588 007 820 606 9	-0.578 509 492 482	-0.569 574 637 54	-0.561 186 505 1
	-0.588 007 820 606 99^d	-0.578 509 492 46	-0.569 574 637 56	-0.561 186 506 35
9	-0.585 850 800 433 7	-0.576 468 380 169	-0.567 645 742 58	-0.559 366 747 1
	-0.585 850 800 433 87^d	-0.576 468 380 15	-0.567 645 742 64	-0.559 366 748 32
10	-0.583 508 206 414 4	-0.574 252 249 872	-0.565 552 133 03	-0.557 392 388 2
	-0.583 508 206 414 57^d	-0.574 252 249 85	-0.565 552 133 10	-0.557 392 389 42
11	-0.580 994 255 517 9	-0.571 874 702 601	-0.563 306 840 95	-0.555 275 937 7
	-0.580 994 255 518 01^d	-0.571 874 702 58	-0.563 306 841 02	-0.555 275 938 84
12	-0.578 323 432 777 8	-0.569 349 597 646	-0.560 923 150 05	-0.553 030 153 2
	-0.578 323 432 777 97^d	-0.569 349 597 61	-0.560 923 150 12	-0.553 030 154 22
13	-0.575 510 306 398 5	-0.566 690 878 119	-0.558 414 431 31	-0.550 667 886 2
	-0.575 510 306 37	-0.566 690 878 11	-0.558 414 431 38	-0.550 667 887 26
14	-0.572 569 366 530 4	-0.563 912 419 513	-0.555 794 001 00	-0.548 201 949 8
	-0.572 569 366 51	-0.563 912 419 49	-0.555 794 001 09	-0.548 201 950 86
15	-0.569 514 888 762 2	-0.561 027 902 144	-0.553 075 001 79	-0.545 645 007 9
	-0.569 514 888 74	-0.561 027 902 14	-0.553 075 001 87	-0.545 645 008 95
16	-0.566 360 822 174 0	-0.558 050 707 254	-0.550 270 306 85	-0.543 009 487 9
	-0.566 360 822 15	-0.558 050 707 24	-0.550 270 306 91	-0.543 009 488 90
17	-0.563 120 700 897 8	-0.554 993 835 680	-0.547 392 445 68	-0.540 307 513 7
	-0.563 120 700 88	-0.554 993 835 67	-0.547 392 445 73	-0.540 307 514 61
18	-0.559 807 577 501 8	-0.551 869 847 486	-0.544 453 550 24	-0.537 550 859 0
	-0.559 807 577 45	-0.551 869 847 45	-0.544 453 550 29	-0.537 550 859 83
19	-0.556 433 976 142 5	-0.548 690 820 585	-0.541 465 319 58	-0.534 750 919 3
	-0.556 433 976 10	-0.548 690 820 57	-0.541 465 319 63	-0.534 750 920 04
20	-0.553 011 863 258 8	-0.545 468 326 311	-0.538 439 001 16	-0.531 918 700 1
	-0.553 011 863 22	-0.545 468 326 30	-0.538 439 001 20	-0.531 918 700 81
21	-0.549 552 633 572 9	-0.542 213 419 906	-0.535 385 387 00	-0.529 064 821 1
	-0.549 552 633 53	-0.542 213 419 86	-0.535 385 387 04	-0.529 064 821 72
22	-0.546 067 109 285 0	-0.538 936 644 076	-0.532 314 823 38	-0.526 199 534 8
	-0.546 067 109 22	-0.538 936 644 05	-0.532 314 823 41	-0.526 199 535 29
23	-0.542 565 550 550 5	-0.535 648 044 025	-0.529 237 232 79	-0.523 332 759 6
	-0.542 565 550 49	-0.535 648 044 01	-0.529 237 232 81	-0.523 332 759 99
24	-0.539 057 675 600 7	-0.532 357 192 725	-0.526 162 147 73	-0.520 474 127 9
	-0.539 057 675 58	-0.532 357 192 68	-0.526 162 147 74	-0.520 474 128 23
25	-0.535 552 689 189 4	-0.529 073 225 592	-0.523 098 756 19	-0.517 633 051 1
	-0.535 552 689 16	-0.529 073 225 56	-0.523 098 756 18	-0.517 633 051 39

Continued on Next Page...

Table 1 – Continuation

L	$v=0$	$v=1$	$v=2$	$v=3$
26	-0.532 059 318 403 4	-0.525 804 884 277	-0.520 055 959 88	-0.514 818 804 7
	-0.532 059 318 34	-0.525 804 884 21	-0.520 055 959 86	-0.514 818 804 90
27	-0.528 585 855 292 2	-0.522 560 569 912	-0.517 042 447 52	-0.512 040 640 1
	-0.528 585 855 25	-0.522 560 569 84	-0.517 042 447 51	-0.512 040 640 25
28	-0.525 140 206 242 8	-0.519 348 407 044	-0.514 066 787 02	-0.509 307 935 1
	-0.525 140 206 16	-0.519 348 407 01	-0.514 066 787 00	-0.509 307 935 21
29	-0.521 729 948 617 0	-0.516 176 320 684	-0.511 137 543 92	-0.506 630 401 9
	-0.521 729 948 55	-0.516 176 320 61	-0.511 137 543 89	-0.506 630 401 96
30	-0.518 362 395 936 9	-0.513 052 130 786	-0.508 263 438 21	-0.504 018 389 9
	-0.518 362 395 87	-0.513 052 130 73	-0.508 263 438 18	-0.504 018 389 91
31	-0.515 044 673 983 8	-0.509 983 671 425	-0.505 453 561 05	-0.501 483 354 1
	-0.515 044 673 92	-0.509 983 671 35	-0.505 453 560 98	-0.501 483 354 05
32	-0.511 783 811 807 3	-0.506 978 947 094	-0.502 717 691 44	-0.499 038 641 7
	-0.511 783 811 71	-0.506 978 947 03	-0.502 717 691 38	-0.499 038 641 65
33	-0.508 586 854 260 8	-0.504 046 347 959	-0.500 066 791 73	-0.496 700 970 5
	-0.508 586 854 19	-0.504 046 347 86	-0.500 066 791 69	-0.496 700 970 47
34	-0.505 461 007 173 3	-0.501 194 964 711	-0.497 513 855 93	-0.494 493 731 1
	-0.505 461 007 08	-0.501 194 964 64	-0.497 513 855 86	-0.494 493 731 12
35	-0.502 413 834 509 9	-0.498 435 084 588	-0.495 075 553 29	-0.492 457
	-0.502 413 834 44	-0.498 435 084 52	-0.495 075 553 22	-0.492 457 8
36	-0.499 453 543 217 6	-0.495 779 051 406	-0.492 776 112	
	-0.499 453 543 14	-0.495 779 051 34	-0.492 776 110 97	
37	-0.496 589 427 076 0	-0.493 242 971 555	-0.490 66	
	-0.496 589 426 96	-0.493 242 971 49	-0.490 660 7	
38	-0.493 832 629 114 0	-0.490 850 95		
	-0.493 832 629 02	-0.490 850 96		
39	-0.491 197 646 03			
	-0.491 197 645 93			
40	-0.488 706 1			
	-0.488 706 110			

Let us start the discussion with the $(L^\pi, v) = (0^+, 0)$ ground state. The energy of the 0^+ ground state has been improved with respect to Moss' result in a number of papers [2, 3, 4, 5, 6, 7, 8] to reach an accuracy around or beyond 30 digits in [7, 8]. Our accuracy is about 10^{-13}. For the $(0^+, 1)$ first vibrational excited state, the accuracy is better than 10^{-11} [7]. For the $(0^+, 2)$ and $(0^+, 3)$ states, the accuracies are about 10^{-10} and 10^{-9}, respectively [3]. There is thus about a one-digit loss for each vibrational excitation. When the numbers of mesh points are increased to $N = 55$ and $N_z = 25$, the accuracies of all these states reach about 10^{-14} (see the third line of the $L = 0$ energies). The

energy of the lowest $L = 1$ state is known with about 25 digits [7, 8]. Our result has an accuracy better than 2×10^{-13}. Comparisons with references [1, 3] indicate that the accuracies of the $L = 1$ vibrational excited states behave like for $L = 0$. Results with an accuracy close to 18 digits are available for $L = 2$-12 and $v = 0$ [11]. They show that our error for the lowest vibrational energy remains smaller than 2×10^{-13} for all these states. When comparing the rest of our results with those of Moss [1], one observes that both works agree very well. We are a little more accurate for $v = 0$ and a little less accurate for $v = 2$ and 3. But in addition, the Lagrange-mesh method provides easy-to-use wave functions. The obtained spectrum is depicted in Fig. 1.

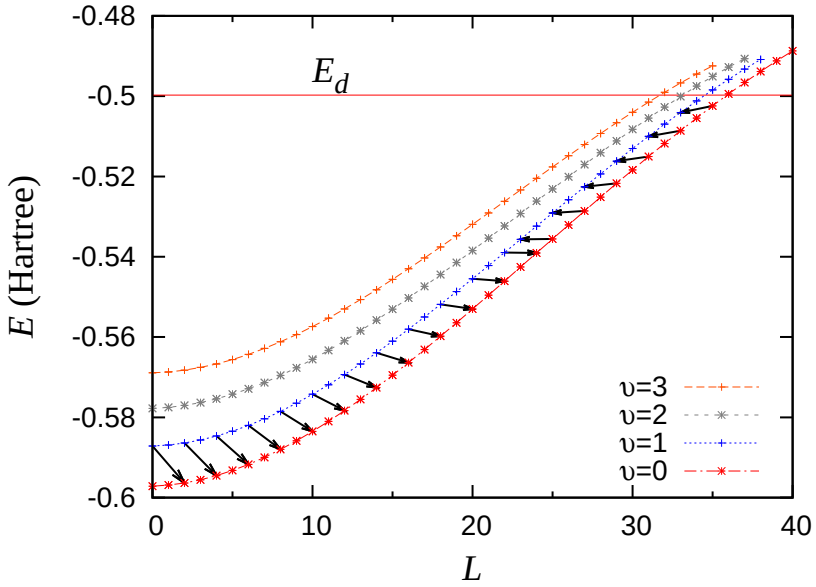

Figure 1. Four lowest Σ_g rotational bands of the H_2^+ molecular ion and dissociation energy E_d. Arrows show how the direction of $L \to L + 2$ transitions between the two lowest bands changes along the band.

Typical convergence tests are displayed in Table 2 for two quite different sets of initial and final states. For the values $h = 0.14$ and $h_z = 0.4$ close to those suggested in [10], Table 2 displays initial and final energies and transition probabilities for various choices of N and N_z. The transition probability W_0 is obtained by restricting (25) to $\kappa = 0$ while W_1 corresponds to $\kappa \leq 1$. First one observes that the $\kappa = 1$ contributions have an importance smaller than 0.05 % and that the $\kappa = 2$ contributions are smaller than 0.001 %. Second one sees that the convergence of the transition probabilities is slower than the convergence of the energies, as expected from the variational principle. A good convergence with respect to N_z is already obtained for $N_z = 20$. The convergence with respect to N is slower. Increasing N is more expensive than increasing N_z since the size of the basis increases with N^2. Since the convergence is exponential, one can estimate that the relative accuracy on W is about 10^{-9} for $(4^+, 0) \to (2^+, 0)$ and still better than 10^{-8} for $(30^+, 2) \to (32^+, 0)$. This means that the wave functions are quite accurate. Further similar tests have been performed for other transitions.

Table 2. Convergence of the energies and transition probabilities as a function of the numbers N and N_z of mesh points. Two cases are shown: $(4^+,0) \rightarrow (2^+,0)$ where $L_f = L_i + 2$ (upper set) and $(30^+,2) \rightarrow (32^+,0)$ where $L_f = L_i - 2$ (lower set). The scale factors are $h = 0.14$ and $h_z = 0.4$.

N	N_z	$E_i(4^+,0)$	$E_f(2^+,0)$	W_0 $(10^{-10}\mathrm{s}^{-1})$	W_1 $(10^{-10}\mathrm{s}^{-1})$	W $(10^{-10}\mathrm{s}^{-1})$
20	20	-0.594 516 6	-0.596 344 6	9.213 5	9.209 8	9.209 8
25	20	-0.594 517 156	-0.596 345 193	9.212 254	9.208 480	9.208 477
30	20	-0.594 517 169 03	-0.596 345 205 26	9.212 220 3	9.208 445 8	9.208 442 3
35	20	-0.594 517 169 315	-0.596 345 205 539	9.212 219 410	9.208 444 904	9.208 441 446
35	30	-0.594 517 169 315	-0.596 345 205 539	9.212 219 411	9.208 444 904	9.208 441 437
40	20	-0.594 517 169 322 29	-0.596 345 205 545 33	9.212 219 383	9.208 444 877	9.208 441 409
40	30	-0.594 517 169 322 30	-0.596 345 205 545 33	9.212 219 384	9.208 444 878	9.208 441 410
[11]		-0.594 517 169 322 41	-0.596 345 205 545 46			
N	N_z	$E_i(30^+,2)$	$E_f(32^+,0)$	W_0 $(10^{-10}\mathrm{s}^{-1})$	W_1 $(10^{-10}\mathrm{s}^{-1})$	W $(10^{-10}\mathrm{s}^{-1})$
20	20	-0.508 07	-0.511 781 9	2.72	2.72	2.72
25	20	-0.508 260 8	-0.511 783 798	2.394 0	2.393 5	2.393 5
30	20	-0.508 263 395	-0.511 783 811 69	2.391 953	2.391 480	2.391 488
35	20	-0.508 263 437 6	-0.511 783 811 805 9	2.391 930 599	2.391 457 162	2.391 465 808
35	30	-0.508 263 437 6	-0.511 783 811 805 9	2.391 930 596	2.391 457 159	2.391 465 806
40	20	-0.508 263 438 21	-0.511 783 811 807 25	2.391 930 370	2.391 456 933	2.391 465 579
40	30	-0.508 263 438 21	-0.511 783 811 807 25	2.391 930 368	2.391 456 931	2.391 465 577
[1]		-0.508 263 438 18	-0.511 783 811 71			

The convergence of the transition probabilities with respect to $K_{\max}$ can be studied by comparison with results from wave functions truncated at $K_{\max} = 0$ and $K_{\max} = 1$. The relative error when $K_{\max} = 0$ is smaller than 0.3 % for all considered transitions while the error for $K_{\max} = 1$ is smaller than 10^{-5}. This is rather similar to truncations with respect to κ. By extrapolation, we estimate that the relative error on the present transition probabilities obtained with $K_{\max} = 2$ should be smaller than 10^{-7}.

The probabilities per second for transitions within a same rotational band, $L_f = L_i - 2$ and $v_f = v_i \leq 3$, are presented in Table 3. They include some transition probabilities involving quasibound states. In accord with the previous discussion, we limit the number of significant figures to six. The probabilities increase slowly with L with a maximum around $L_i = 32$ for $v_i = 0$, $L_i = 30$ for $v_i = 1$, $L_i = 28$ for $v_i = 2$, and $L_i = 27$ for $v_i = 3$, not far from the end of the rotational bands. This is due to a maximum of the energy differences around $L_i = 25$. The maximum of the transition probabilities is shifted toward higher L_i values by a steady increase of the reduced matrix elements. The transition probabilities behave similarly for the displayed v values with a slight decrease when v increases.

Table 3: Quadrupole transition probabilities per second W for transitions between states of a same rotational band ($v_f = v_i$, $L_f = L_i - 2$). Results are given with five digits followed by the power of 10.

L_i	$v_i = 0$	$v_i = 1$	$v_i = 2$	$v_i = 3$
2	9.731 37-12	9.680 53-12	9.441 58-12	9.038 44-12
3	1.581 33-10	1.570 47-10	1.529 34-10	1.461 88-10
4	9.208 44-10	9.122 85-10	8.863 66-10	8.454 10-10
5	3.316 04-09	3.274 74-09	3.172 19-09	3.016 92-09
6	9.003 66-09	8.856 98-09	8.548 31-09	8.101 26-09
7	2.027 18-08	1.985 14-08	1.907 78-08	1.800 55-08
8	3.991 47-08	3.888 76-08	3.719 19-08	3.493 66-08
9	7.102 43-08	6.880 86-08	6.545 68-08	6.116 68-08
10	1.167 28-07	1.124 01-07	1.063 06-07	9.877 20-08
11	1.799 09-07	1.721 22-07	1.617 76-07	1.493 87-07
12	2.629 44-07	2.498 55-07	2.332 90-07	2.140 06-07
13	3.674 92-07	3.467 23-07	3.214 91-07	2.928 58-07
14	4.943 34-07	4.629 69-07	4.261 64-07	3.853 47-07
15	6.432 99-07	5.979 13-07	5.462 22-07	4.900 73-07
16	8.132 46-07	7.499 75-07	6.797 55-07	6.049 01-07
17	1.002 12-06	9.167 53-07	8.241 37-07	7.270 87-07
18	1.207 04-06	1.095 14-06	9.761 56-07	8.534 13-07
19	1.424 45-06	1.281 49-06	1.132 17-06	9.803 47-07
20	1.650 27-06	1.471 75-06	1.288 26-06	1.104 19-06
21	1.880 04-06	1.661 62-06	1.440 38-06	1.221 22-06
22	2.109 12-06	1.846 74-06	1.584 53-06	1.327 83-06
23	2.332 81-06	2.022 80-06	1.716 79-06	1.420 58-06
24	2.546 48-06	2.185 62-06	1.833 51-06	1.496 35-06
25	2.745 72-06	2.331 32-06	1.931 34-06	1.552 32-06
26	2.926 40-06	2.456 32-06	2.007 25-06	1.586 08-06
27	3.084 74-06	2.557 42-06	2.058 62-06	1.595 57-06
28	3.217 37-06	2.631 82-06	2.083 22-06	1.579 13-06
29	3.321 35-06	2.677 12-06	2.079 17-06	1.535 44-06
30	3.394 20-06	2.691 32-06	2.044 95-06	1.463 47-06
31	3.433 83-06	2.672 76-06	1.979 30-06	1.362 40-06
32	3.438 58-06	2.620 08-06	1.881 15-06	1.231 41-06
33	3.407 11-06	2.532 10-06	1.749 39-06	1.069 27-06
34	3.338 37-06	2.407 67-06	1.582 54-06	8.732 11-07
35	3.231 44-06	2.245 36-06	1.377 99-06	6.32 -07
36	3.085 37-06	2.042 91-06	1.129 4 -06	

Continued on Next Page...

Table 3 – Continuation

L_i	$v_i = 0$	$v_i = 1$	$v_i = 2$	$v_i = 3$
37	2.898 82-06	1.795 86-06	8.1 -07	
38	2.669 34-06	1.492 9 -06		
39	2.391 63-06			
40	2.051 -06			

The probabilities per second for other transitions are displayed in Table 4. The columns correspond to transitions between different vibrational states. For each L_i value, the successive lines correspond to increasing values of L_f, i.e., to $L_f = L_i - 2$ for $L_i > 1$, $L_f = L_i$ for $L_i > 0$, and $L_f = L_i + 2$, respectively. For $L_i \leq 20$, the obtained probabilities agree with those of Posen *et al* [13] and improve them significantly. More than 95 % of the results of Posen *et al* exactly correspond to our result rounded at two significant figures. In most other cases, the rounding is of 6 units on the third digit rather than at most 5 for a normal rounding. An example of the few 'worst' cases is the $(19^-, 3) \rightarrow (17^-, 2)$ transition probability where our result in Table 4 is $5.847\,00 \times 10^{-10}$ while the result of Posen *et al* is 5.7×10^{-10}.

The strongest transition from each state occurs in general towards the nearest vibrational state ($v_f = v_i - 1$) for $L_f = L_i - 2$. Exceptions can be found between $L_i = 14$ and $L_i = 22$. For $v_f = v_i - 1$, in the vicinity of $L_i = 23$ and beyond, the $(L_i, v_i) \rightarrow (L_i + 2, v_i - 1)$ transitions are replaced by $(L_i + 2, v_i - 1) \rightarrow (L_i, v_i)$ transitions because the sign of the energy difference changes (see the arrows in Fig. 1 for the $1 \rightarrow 0$ transitions). These numbers are indicated in italics in Table 4. For example, the first number in the last line for $L_i = 23$ corresponds to the $(25, 0) \rightarrow (23, 1)$ transition. Hence the transition probabilities strongly vary in this region.

Table 4: Quadrupole transition probabilities per second W for transitions between different vibrational quantum numbers ($v_i \neq v_f$). The three successive lines correspond to increasing L_f values, i.e. $L_f = L_i - 2$, $L_f = L_i$ and $L_f = L_i + 2$, respectively, for $L_i \geq 2$. Italicized numbers for $(1 \rightarrow 0)$, $(2 \rightarrow 1)$ and $(3 \rightarrow 2)$ mean that the initial and final states are exchanged (the first one is preceded in each case by a horizontal bar).

L_i	$(1 \rightarrow 0)$	$(2 \rightarrow 0)$	$(2 \rightarrow 1)$	$(3 \rightarrow 0)$	$(3 \rightarrow 1)$	$(3 \rightarrow 2)$
0	5.215 07-07	6.777 83-08	8.571 80-07	6.277 98-09	1.780 77-07	1.045 81-06
1	2.649 11-07	4.310 45-08	4.326 10-07	5.534 79-09	1.103 90-07	5.244 04-07
	2.586 05-07	2.801 60-08	4.263 10-07	1.845 73-09	7.518 42-08	5.215 85-07
2	1.602 07-07	3.128 77-08	2.593 97-07	4.978 71-09	7.845 99-08	3.117 14-07
	1.878 56-07	3.070 72-08	3.066 23-07	3.960 55-09	7.859 99-08	3.714 70-07

Continued on Next Page...

Table 4 – Continuation

L_i	$(1 \to 0)$	$(2 \to 0)$	$(2 \to 1)$	$(3 \to 0)$	$(3 \to 1)$	$(3 \to 2)$
	1.788 44-07	1.552 08-08	2.953 94-07	5.794 07-10	4.279 53-08	3.620 35-07
3	2.266 89-07	4.932 77-08	3.644 12-07	8.766 41-09	1.221 20-07	4.346 60-07
	1.734 34-07	2.854 37-08	2.828 71-07	3.705 83-09	7.300 64-08	3.423 98-07
	1.303 97-07	8.543 49-09	2.155 75-07	9.058 65-11	2.444 93-08	2.643 79-07
4	2.707 32-07	6.511 44-08	4.315 88-07	1.270 26-08	1.592 35-07	5.102 93-07
	1.664 90-07	2.764 82-08	2.712 73-07	3.620 52-09	7.064 46-08	3.279 79-07
	9.561 75-08	4.302 52-09	1.580 64-07	6.224 68-12	1.302 46-08	1.937 59-07
5	3.014 07-07	7.967 25-08	4.758 87-07	1.685 06-08	1.925 14-07	5.569 65-07
	1.613 88-07	2.709 90-08	2.626 29-07	3.585 87-09	6.915 50-08	3.170 65-07
	6.941 20-08	1.811 97-09	1.146 16-07	1.565 94-10	6.048 80-09	1.402 78-07
6	3.207 99-07	9.285 79-08	5.009 67-07	2.109 87-08	2.217 19-07	5.794 49-07
	1.567 37-07	2.666 41-08	2.546 75-07	3.571 42-09	6.794 44-08	3.069 22-07
	4.952 07-08	5.182 10-10	8.159 26-08	4.325 02-10	2.152 92-09	9.958 45-08
7	3.294 90-07	1.042 47-07	5.081 31-07	2.527 53-08	2.459 44-07	5.797 94-07
	1.520 72-07	2.626 02-08	2.466 56-07	3.565 77-09	6.680 07-08	2.966 42-07
	3.456 91-08	3.448 24-11	5.676 83-08	7.573 73-10	3.815 77-10	6.900 63-08
8	3.278 82-07	1.133 81-07	4.984 70-07	2.918 88-08	2.642 39-07	5.598 86-07
	1.472 13-07	2.585 04-08	2.382 86-07	3.563 40-09	6.563 11-08	2.858 90-07
	2.353 32-08	6.950 92-11	3.846 88-08	1.078 40-09	9.972 57-12	4.650 68-08
9	3.166 31-07	1.198 77-07	4.735 30-07	3.265 26-08	2.758 66-07	5.222 05-07
	1.420 95-07	2.541 62-08	2.294 66-07	3.561 15-09	6.438 97-08	2.745 59-07
	1.557 36-08	4.029 37-10	2.530 54-08	1.361 71-09	4.833 24-10	3.037 65-08
10	2.967 79-07	1.234 84-07	4.354 87-07	3.550 39-08	2.804 30-07	4.699 78-07
	1.367 05-07	2.494 77-08	2.201 84-07	3.556 97-09	6.305 21-08	2.626 41-07
	9.984 06-09	8.730 29-10	1.609 93-08	1.588 31-09	1.388 38-09	1.915 21-08
11	2.697 51-07	1.241 05-07	3.871 01-07	3.761 71-08	2.779 21-07	4.070 73-07
	1.310 56-07	2.443 93-08	2.104 68-07	3.549 43-09	6.160 56-08	2.501 85-07
	6.174 74-09	1.367 15-09	9.861 25-09	1.750 47-09	2.431 87-09	1.159 85-08
12	2.372 84-07	1.218 08-07	3.315 58-07	3.891 19-08	2.687 08-07	3.377 66-07
	1.251 76-07	2.388 83-08	2.003 72-07	3.537 51-09	6.004 43-08	2.372 66-07
	3.664 57-09	1.812 72-09	5.781 88-09	1.848 36-09	3.419 76-09	6.703 66-09
13	2.013 14-07	1.168 10-07	2.722 68-07	3.935 61-08	2.534 97-07	2.664 61-07
	1.191 02-07	2.329 38-08	1.899 63-07	3.520 50-09	5.836 71-08	2.239 77-07
	2.072 49-09	2.168 45-09	3.220 15-09	1.887 28-09	4.236 60-09	3.666 07-09
14	1.638 56-07	1.094 48-07	2.126 54-07	3.896 32-08	2.332 57-07	1.974 23-07
	1.128 75-07	2.265 65-08	1.793 15-07	3.497 94-09	5.657 63-08	2.104 17-07
	1.106 44-09	2.416 35-09	1.685 68-09	1.875 42-09	4.826 21-09	1.874 47-09
15	1.268 86-07	1.001 55-07	1.559 56-07	3.778 72-08	2.091 41-07	1.345 41-07
	1.065 38-07	2.197 77-08	1.685 05-07	3.469 59-09	5.467 65-08	1.966 90-07

Continued on Next Page...

Table 4 – Continuation

L_i	$(1 \to 0)$	$(2 \to 0)$	$(2 \to 1)$	$(3 \to 0)$	$(3 \to 1)$	$(3 \to 2)$
	5.503 02-10	2.554 61-09	8.171 40-10	1.822 20-09	5.174 46-09	8.808 62-10
16	9.223 82-08	8.942 07-08	1.050 69-07	3.591 44-08	1.823 95-07	8.114 32-08
	1.001 36-07	2.125 98-08	1.576 12-07	3.435 36-09	5.267 42-08	1.829 00-07
	2.501 72-10	2.591 95-09	3.588 70-10	1.737 09-09	5.294 99-09	3.708 12-10
17	6.152 63-08	7.775 80-08	6.243 16-08	3.345 47-08	1.542 90-07	3.987 69-08
	9.371 07-08	2.050 57-08	1.467 11-07	3.395 33-09	5.057 72-08	1.691 46-07
	1.009 96-10	2.543 02-09	1.380 41-10	1.628 96-09	5.217 88-09	1.342 71-10
18	3.608 52-08	6.567 76-08	2.994 76-08	3.053 21-08	1.260 48-07	1.264 35-08
	8.730 54-08	1.971 86-08	1.358 76-07	3.349 67-09	4.839 45-08	1.555 25-07
	3.456 07-11	2.425 16-09	4.397 10-11	1.505 59-09	4.981 25-09	3.900 66-11
19	1.694 12-08	5.366 17-08	8.957 52-09	2.727 70-08	9.879 86-08	5.847 00-10
	8.095 94-08	1.890 20-08	1.251 77-07	3.298 61-09	4.613 53-08	1.421 29-07
	9.236 20-12	2.256 10-09	1.046 55-11	1.373 54-09	4.625 31-09	7.945 85-12
20	4.801 86-09	4.214 82-08	2.402 42-10	2.381 90-08	7.353 80-08	4.109 05-09
	7.471 00-08	1.805 97-08	1.146 77-07	3.242 44-09	4.380 95-08	1.290 40-07
	1.634 20-12	2.052 46-09	1.491 48-12	1.238 14-09	4.188 47-09	8.263 64-13
21	6.367 84-11	3.151 84-08	4.042 78-09	2.028 15-08	5.111 21-08	2.294 84-08
	6.859 13-08	1.719 52-08	1.044 37-07	3.181 49-09	4.142 69-08	1.163 35-07
	1.257 21-13	1.828 90-09	6.692 18-14	1.103 56-09	3.705 00-09	1.417 34-14
22	2.833 83-09	2.209 23-08	2.012 90-08	1.677 84-08	3.220 67-08	5.623 30-08
	6.263 42-08	1.631 23-08	9.450 89-08	3.116 02-09	3.899 71-08	1.040 85-07
	6.603 90-16	1.597 74-09	8.018 89-18	9.729 19-10	3.203 89-09	*6.866 45-18*
23	1.296 07-08	1.412 66-08	4.783 98-08	1.341 17-08	1.735 01-08	1.025 75-07
	5.686 63-08	1.541 45-08	8.494 09-08	3.046 28-09	3.652 98-08	9.234 86-08
	2.025 61-16	1.368 88-09	*7.058 38-15*	8.484 91-10	2.708 50-09	*7.298 79-14*
24	3.006 99-08	7.818 20-09	8.615 82-08	1.027 11-08	6.922 56-09	1.601 54-07
	5.131 20-08	1.450 52-08	7.577 44-08	2.972 44-09	3.403 39-08	8.118 05-08
	6.639 13-14	1.149 88-09	*3.825 31-13*	7.318 12-10	2.236 72-09	*1.475 85-12*
25	5.360 26-08	3.308 86-09	1.337 74-07	7.434 48-09	1.170 61-09	2.267 95-07
	4.599 22-08	1.358 74-08	6.704 54-08	2.894 56-09	3.151 83-08	7.062 60-08
	8.591 82-13	9.462 12-10	*3.286 54-12*	6.238 49-10	1.801 45-09	*9.232 71-12*
26	8.285 30-08	6.929 09-10	1.891 45-07	4.969 60-09	2.243 78-10	3.000 34-07
	4.092 49-08	1.266 43-08	5.878 42-08	2.812 55-09	2.899 09-08	6.072 32-08
	4.483 42-12	7.615 46-10	*1.433 78-11*	5.251 26-10	1.411 26-09	*3.453 91-11*
27	1.170 03-07	2.547 68-11	2.505 47-07	2.936 77-09	4.115 31-09	3.771 70-07
	3.612 48-08	1.173 84-08	5.101 58-08	2.726 10-09	2.645 96-08	5.150 34-08
	1.515 17-11	5.980 33-10	*4.393 05-11*	4.358 31-10	1.071 06-09	*9.690 71-11*
28	1.551 55-07	1.331 45-09	3.161 14-07	1.392 31-09	1.279 22-08	4.552 88-07
	3.160 38-08	1.081 22-08	4.376 02-08	2.634 66-09	2.393 13-08	4.299 11-08

Continued on Next Page...

Table 4 – Continuation

L_i	$(1 \rightarrow 0)$	$(2 \rightarrow 0)$	$(2 \rightarrow 1)$	$(3 \rightarrow 0)$	$(3 \rightarrow 1)$	$(3 \rightarrow 2)$
	3.973 15-11	4.566 04-10	*1.085 29-10*	3.559 08-10	7.827 86-10	*2.267 22-10*
29	1.963 55-07	4.614 58-09	3.838 68-07	3.931 96-10	2.613 24-08	5.312 52-07
	2.737 13-08	9.887 88-09	3.703 24-08	2.537 30-09	2.141 25-08	3.520 44-08
	8.836 10-11	3.372 29-10	*2.323 95-10*	2.851 33-10	5.460 45-10	*4.691 66-10*
30	2.396 14-07	9.866 27-09	4.517 18-07	2.792 67-12	4.394 41-08	6.016 44-07
	2.343 40-08	8.967 20-09	3.084 36-08	2.432 53-09	1.890 86-08	2.815 61-08
	1.753 59-10	2.391 47-10	*4.503 88-10*	2.231 64-10	3.586 27-10	*8.911 70-10*
31	2.839 17-07	1.707 35-08	5.174 45-07	2.981 56-10	6.594 74-08	6.626 16-07
	1.979 66-08	8.051 67-09	2.520 07-08	2.318 03-09	1.642 37-08	2.185 36-08
	3.207 59-10	1.610 56-10	*8.129 59-10*	1.695 91-10	2.169 60-10	*1.594 77-09*
32	3.282 30-07	2.622 48-08	5.786 27-07	1.378 71-09	9.170 79-08	7.095 59-07
	1.646 15-08	7.142 29-09	2.010 72-08	2.190 00-09	1.395 93-08	1.629 95-08
	5.530 23-10	1.012 66-10	*1.395 55-09*	1.239 65-10	1.164 28-10	*2.744 97-09*
33	3.714 82-07	3.730 98-08	6.324 92-07	3.373 48-09	1.204 39-07	7.363 38-07
	1.342 94-08	6.239 26-09	1.556 31-08	2.041 80-09	1.151 08-08	1.149 16-08
	9.140 72-10	5.780 87-11	*2.317 44-09*	8.581 12-11	5.155 74-11	*4.635 39-09*
34	4.125 30-07	5.030 24-08	6.755 69-07	6.427 78-09	1.503 43-07	7.331 27-07
	1.069 95-08	5.341 33-09	1.156 57-08	1.859 72-09	9.057 10-09	7.421 17-09
	1.469 02-09	2.850 59-11	*3.783 25-09*	5.463 02-11	1.598 07-11	*7.879 45-09*
35	4.500 71-07	6.508 15-08	7.028 51-07	1.05 -08	1.75 -07	6.76 -07
	8.269 35-09	4.443 93-09	8.108 79-09	1.60 -09	6.49 -09	4.05 -09
	2.326 54-09	1.097 77-11	*6.188 39-09*	2.97 -11	2.05 -12	*1.4 -08*
36	4.824 27-07	8.108 3 -08	7.051 4 -07			
	6.135 07-09	3.532 6 -09	5.179 8 -09			
	3.686 47-09	2.566 2 -12	*1.046 7 -08*			
37	5.069 63-07	9.4 -08	6.5 -07			
	4.291 06-09	2.5 -09	2.7 -09			
	5.971 46-09	1.3 -13				
38	5.179 -07					
	2.727 -09					
	1.033 -08					

Oscillator strengths are depicted in Figs. 2, 3 and 4. For the transitions with $\Delta L = L_i - L_f = -2$ displayed in Fig. 2, they present a strong variation along the band. They also vary strongly with $\Delta v = v_i - v_f$. The $\Delta v = 1$ transitions present a deep minimum around $L_i = 23$ due to the change of sign of the energy difference (see Fig. 1). Beyond that value, the initial state is lower than the final $v_f < v_i$ state and the strengths are negative. Otherwise the strengths slowly increase with the vibrational excitation. The $\Delta v = 2$ strengths are smaller by more than an order of magnitude. The minimum

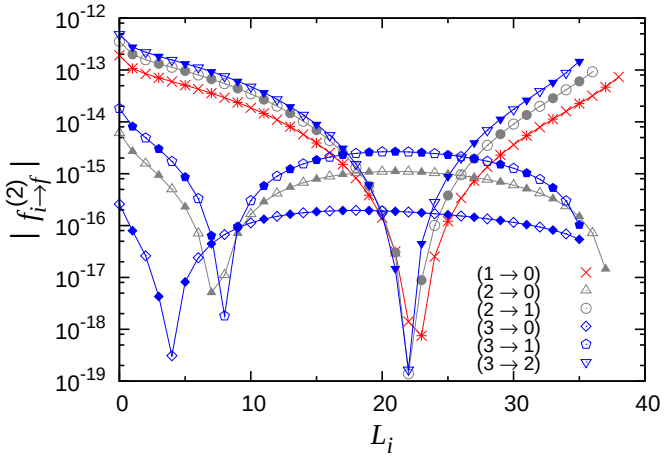

Figure 2. Oscillator strengths for $L_f = L_i + 2$ transitions.

occurring around $L_i = 8$ is here due to a change of sign of the matrix element appearing in (3). The $\Delta v = 3$ strengths are smaller by more than an order of magnitude than the $\Delta v = 2$ strengths. Except near the minimum at $L_i = 4$ also due to a change of sign of the matrix element, they are rather constant along the band.

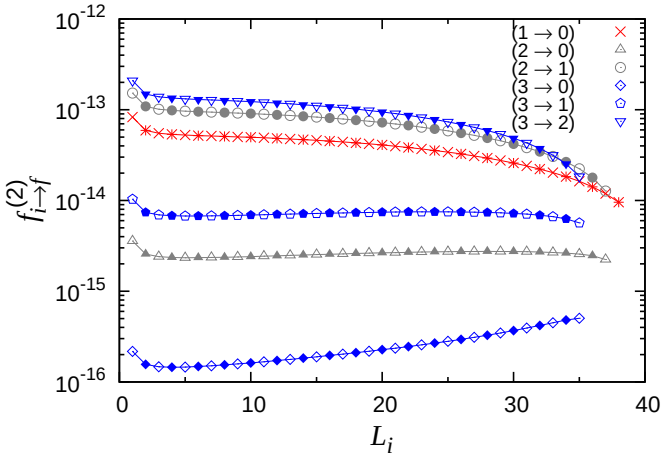

Figure 3. Oscillator strengths for $L_f = L_i$ transitions.

The $\Delta L = 0$ oscillator strengths presented in Fig. 3 do not vary much along the bands as expected from the similar vibrational structures of the initial and final states. They slowly decrease for $\Delta v = 1$ and slowly increase for $\Delta v = 3$. They are remarkably flat for $\Delta v = 2$. Except near the end of the band, for given Δv, they increase with v.

The $\Delta L = +2$ strengths presented in Fig. 4 behave similarly to the $\Delta L = -2$ strengths. Minima take place around $L_i = 20$ for $\Delta v = 1$, $L_i = 26$ for $\Delta v = 2$ and $L_i = 30$ for $\Delta v = 3$. These minima thus occur now at increasing L_i values with increasing Δv and are all due to a change of sign of the matrix element.

Lifetimes are defined as

$$\tau = \Big(\sum_{E_f < E_i} W_{i\to f} \Big)^{-1}. \tag{33}$$

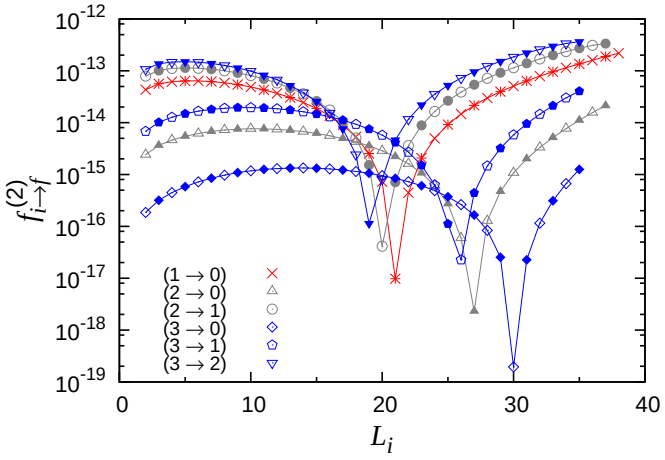

Figure 4. Oscillator strengths for $L_f = L_i - 2$ transitions.

For the $L = 0$ vibrational states, they have been calculated in [33]. The values 1.92×10^6 s, 1.08×10^6 s and 0.813×10^6 s for the first, second and third $L = 0$ excited vibrational states agree respectively well with our values $1.917\,518 \times 10^6$ s, $1.081\,130 \times 10^6$ s and $0.812\,900 \times 10^6$ s obtained from Table 4. Lifetimes for the calculated states are displayed in Fig. 5. For the $(1^-, 0)$ state, the lifetime is infinite within the present description. The large difference between the lifetimes of the $(2^+, 0)$ state and, for example, the $(0^+, 1)$ state is essentially due to the factor $(E_i - E_f)^5$ in expression (7) of the E2 transition probability. Indeed the vibrational energy difference in the transition from the $(0^+, 1)$ state is about 10 times larges than the rotational energy difference in the transition from the $(2^+, 0)$ state which leads to an order of magnitude of 10^5 for the ratio of the lifetimes.

Except for the ground-state rotational band, where the lifetimes decrease rather fast from the very high values obtained at low orbital momenta (about 3300 years for $L = 2$), the lifetimes do not depend much on L. They are rather constant up to about $L = 15$. Then they slowly decrease till about $L = 30$ before starting increasing again slowly. The decrease is less than a factor of five for $v = 1$, three for $v = 2$ and two for $v = 3$. For $v = 1$, the lifetimes are of the order of twenty-two days at small L and of four days near $L = 30$. When v increases from 1 to 3, they decrease progressively for $L \leq 18$ and increase progressively for $L > 18$.

4. Conclusion

In this paper, by accurately solving a three-body Schrödinger equation with Coulomb potentials, we have calculated the energies and wave functions of up to four of the lowest vibrational bound or quasibound states of the hydrogen molecular ion from $L = 0$ to 40. The calculation is performed in perimetric coordinates with the Lagrange-mesh method. For low orbital momenta, a comparison with more accurate calculations in the literature and a cross comparison with the extensive results of Moss [1] show that the

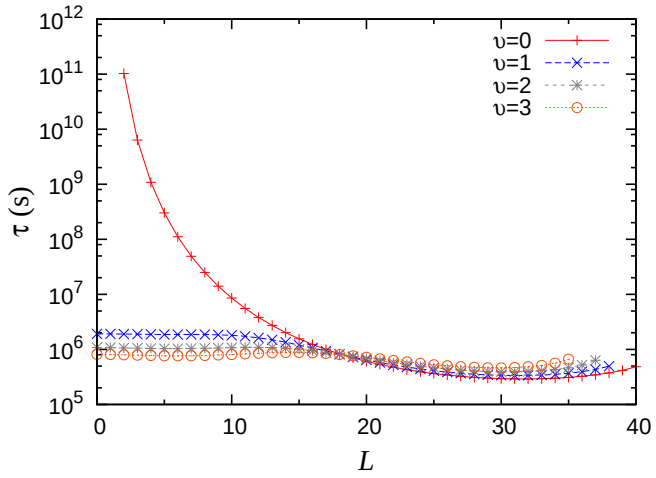

Figure 5. Lifetimes τ in the first four rotational bands ($v = 0 - 3$).

energies with 40 mesh points for the x and y coordinates and 20 mesh points for the z coordinate have an accuracy of about 13 digits for the lowest vibrational state and a slowly decreasing accuracy with vibrational excitation providing still at least 9 digits for the third excited vibrational state. These accuracies are maintained along the whole rotational bands.

With the corresponding wave functions, a simple calculation using the associated Gauss-Laguerre quadrature provides the quadrupole strengths and transition probabilities per time unit over the whole rotational bands. Tests with increasing numbers of mesh points and various truncations on K show that the accuracy on this probabilities should reach six significant figures. The $K = 0$ approximation leads to an error smaller than 0.3 %. It slightly differs from the Born-Oppenheimer approximation by the fact that the proton mass is taken into account here. For the calculated states, we display tables extending the results and improving the accuracy of [13]. Although the displayed accuracy may exceed what is needed in applications, the results can also serve as a benchmark for testing approximate wave functions of H_2^+. Except for the states in the ground-state rotational band that can only decay slowly to the $L_f = L_i - 2$ previous state, all calculated lifetimes have an order of magnitude around 10^6 s.

Acknowledgments

We thank Michel Hesse for information about the codes. This text presents research results of the interuniversity attraction pole programme P6/23 initiated by the Belgian-state Federal Services for Scientific, Technical and Cultural Affairs. H.O.P. thanks CONACyT (México) for a postdoctoral grant.

References

[1] Moss R 1993 *Mol. Phys.* **80** 1541

[2] Korobov V I 2000 *Phys. Rev. A* **61** 064503
[3] Hilico L, Billy N, Grémaud B and Delande D 2000 *Eur. Phys. J. D* **12** 449
[4] Bailey D H and Frolov A M 2002 *J. Phys. B: At. Mol. Opt. Phys.* **35** 4287
[5] Yan Z C, Zhang J Y and Li Y 2003 *Phys. Rev. A* **67** 062504
[6] Cassar M M and Drake G W F 2004 *J. Phys. B: At. Mol. Opt. Phys.* **37** 2485
[7] Li H, Wu J, Zhou B L, Zhu J M and Yan Z C 2007 *Phys. Rev. A* **75** 012504
[8] Hijikata Y, Nakashima H and Nakatsuji H 2009 *J. Chem. Phys.* **130** 024102
[9] Carbonell J, Lazauskas R, Delande D, Hilico L and Kilic S 2003 *Europhys. Lett.* **64** 316
[10] Hesse M and Baye D 2003 *J. Phys. B: At. Mol. Opt. Phys.* **36** 139
[11] Yan Z C and Zhang J Y 2004 *J. Phys. B: At. Mol. Opt. Phys.* **37** 1055
[12] Bates D R and Poots G 1953 *Proc. Phys. Soc. A* **66** 784
[13] Posen A, Dalgarno A and Peek J 1983 *At. Data Nucl. Data Tables* **28** 265
[14] Hesse M and Baye D 1999 *J. Phys. B: At. Mol. Opt. Phys.* **32** 5605
[15] Hesse M and Baye D 2001 *J. Phys. B: At. Mol. Opt. Phys.* **34** 1425
[16] Baye D and Heenen P-H 1986 *J. Phys. A: Math. Gen.* **19** 2041
[17] Baye D 2006 *Phys. Stat. Sol. (b)* **243** 1095
[18] Baye D, Hesse M and Vincke M 2002 *Phys. Rev. E* **65** 026701
[19] Baye D, Vincke M and Hesse M 2008 *J. Phys. B: At. Mol. Opt. Phys.* **41** 185002
[20] Baye D, Hesse M and Vincke M 2008 *J. Phys. B: At. Mol. Opt. Phys.* **41** 185002
[21] Baye D and Sparenberg J-M 2010 *Phys. Rev. E* **82** 056701
[22] Vincke M and Baye D 2006 *J. Phys. B: At. Mol. Opt. Phys.* **39** 2605
[23] Olivares-Pilón H, Baye D, Turbiner A V and López Vieyra J C *J. Phys. B: At. Mol. Opt. Phys.* **43** 065702
[24] Descouvemont P, Daniel C and Baye D 2003 *Phys. Rev. C* **67** 044309
[25] Descouvemont P, Tursunov E M and Baye D 2006 *Nucl. Phys. A* **765** 370
[26] Druet T, Baye D, Descouvemont P and Sparenberg J-M 2010 *Nucl. Phys. A* **845** 88
[27] Pekeris C L 1958 *Phys. Rev.* **112** 1649
[28] Sobelman I I 1972 *An Introduction to the Theory of Atomic Spectra* (Pergamon, Oxford)
[29] Sobelman I I 1979 *Atomic Spectra and Radiative Transitions* (Springer, Berlin)
[30] Edmonds A R 1957 *Angular Momentum in Quantum Mechanics* (Princeton, New Jersey)
[31] Feagin J M 1984 *J. Phys. B: At. Mol. Phys.* **17** 2433
[32] Bollhöfer M and Notay Y 2007 *Comput. Phys. Commun.* **177** 951
[33] Peek J M, Hashemi-Attar A R and Beckel C L 1979 *J. Chem. Phys.* **71** 5382